RSC Advances

RSC Publishing

PAPER

View Article Online
View Journal | View Issue

Simple multi-level microchannel fabrication by pseudo-grayscale backside diffused light lithography†

Cite this: *RSC Advances*, 2013, **3**, 19467

David Lai,[ab] Joseph M. Labuz,[a] Jiwon Kim,[bc] Gary D. Luker,[ade] Ariella Shikanov[abc] and Shuichi Takayama*[abcf]

Received 21st April 2013,
Accepted 29th July 2013

DOI: 10.1039/c3ra43834a

www.rsc.org/advances

Photolithography of multi-level channel features in microfluidics is laborious and/or costly. Grayscale photolithography is mostly used with positive photoresists and conventional front side exposure, but the grayscale masks needed are generally costly and positive photoresists are not commonly used in microfluidic rapid prototyping. Here we introduce a simple and inexpensive alternative that uses pseudo-grayscale (pGS) photomasks in combination with backside diffused light lithography (BDLL) and the commonly used negative photoresist, SU-8. BDLL can produce smooth multi-level channels of gradually changing heights without use of true grayscale masks because of the use of diffused light. Since the exposure is done through a glass slide, the photoresist is cross-linked from the substrate side up enabling well-defined and stable structures to be fabricated from even unspun photoresist layers. In addition to providing unique structures and capabilities, the method is compatible with the ''garage microfluidics'' concept of creating useful tools at low cost since pGS BDLL can be performed with the use of only hot plates and a UV transilluminator: equipment commonly found in biology labs. Expensive spin coaters or collimated UV aligners are not needed. To demonstrate the applicability of pGS BDLL, a variety of weir-type cell traps were constructed with a single UV exposure to separate cancer cells (MDA-MB-231, 10–15 μm in size) from red blood cells (RBCs, 2–8 μm in size) as well as follicle clusters (40–50 μm in size) from cancer cells (MDA-MB-231, 10–15 μm in size).

Introduction

The direction of microfluidics as a field is toward more complex operations, and complexity embedded within the device design is especially attractive. Multi-level channel designs have useful applications in microfluidic devices to embed complex operations into the device while insulating the complexity from the user (no need for additional external controls and robust function). Such multi-level channel designs have been used for chaotic mixers,[1] weir-type cell traps for cell isolation,[2] and weir-type cell traps for cell fusion.[3] The lack of moving parts allows for simple operation, however typical applications of such microfluidic devices necessitate the rapid-prototyping process to be quick and cost efficient.

Fabrication of multi-level channel features in microfluidics typically requires multiple exposures where each layer is serially spun, each photomask precisely aligned, and exposed by ultraviolet (UV) light. Alternative methods of producing multi-level channels such as hot embossing,[4] erosion,[5] etching,[6] laser fabrication,[7] photoresist reflow,[8] micro-milling,[9] 3D-printing,[10] electroplating,[11] deformable molds,[12] and liquid molding[13] are also laborious and/or require specialized equipment.

The intrinsic limitation of typical photomask-based photoresist patterning methods is the binary nature of an all-or-none illumination of exposed areas. Thus, many groups have used grayscale photomasks to generate a range of illumination densities using a single exposure. Grayscale photolithography suffers from high costs because grayscale photomasks are generated using scanning lasers,[14] ultra-high resolution binary masks,[15] variable Inconel deposition on glass,[16] or High-Energy Beam Sensitive (HEBS) glass.[17] Low-cost alternatives to grayscale photolithography are complex, requiring the use of a microfluidic photomask.[18] Most grayscale photolithography use positive photoresists[14–18] that are less common in microfluidic device fabrication. Negative photoresists have been used in conjunction with grayscale exposure techniques, however the resulting channels were of low resolution and on the order of milimetres.[19] Others have used negative photoresists for multi-level photolithography with the use of 3D diffusers[20] and digital micro-mirror devices.[21] However each study was either unable to fabricate multi-level features

[a]*Department of Biomedical Engineering, University of Michigan, Ann Arbor, MI, USA*
[b]*Reproductive Sciences Program, University of Michigan, Ann Arbor, MI, USA*
[c]*Department of Macromolecular Science and Engineering, University of Michigan, Ann Arbor, MI, USA*
[d]*Department of Radiology, University of Michigan, Ann Arbor, MI, USA*
[e]*Department of Microbiology and Immunology, University of Michigan, Ann Arbor, MI, USA*
[f]*Division of Nano-Bio and Chemical Engineering WCU Project, UNIST, Ulsan, Republic of Korea. E-mail: takayama@umich.edu*

† Electronic supplementary information (ESI) available: Higher magnification SEM image of pGS BDLL SU-8 molds. See DOI: 10.1039/c3ra43834a

independent of feature width in a single exposure or required a relatively sophisticated semiconductor mask that may deter non-microfluidic scientists from adopting microfluidic technology. BDLL has been used to create microfluidic devices with bell-shaped cross-section microchannels[22] and multi-layered orifices with disconnected photomask features.[23] While this technology has been capable of fine control of short-range tapering and orifice heights, the method has lacked the ability to sustain long channels of varying height. BDLL with pGS photomasks overcomes this shortcoming while maintaining cost-effectiveness and simplicity for the fabrication of microfluidic devices in a single UV exposure.

Cell separation by size is applicable to cancer research for uses including identification of metastatic cancer cells in blood[24] and separation of cancer cells from follicles in oncofertility preservation for young women.[25,26] We use pGS BDLL as a tool to create multi-level weir-type cell traps using only equipment commonly found in many biology labs. This technology increases the accessibility of microfluidics, making a powerful and ever-expanding tool chest of experimental techniques available to more researchers in multiple fields.

Results and discussion

Characterization of pGS BDLL

pGS BDLL is capable of producing multi-level microfluidic devices at superior levels of cost-efficiency and simplicity over conventional photolithography, alternative multi-level fabrication techniques and previous grayscale photomask technologies. A relatively low-cost, low-resolution photomask printed on transparency sheets was used to create an isotropic pattern of binary opaque and transparent 10 by 10 μm squares to produce channels of different heights by BDLL with SU-8 negative photoresist (Fig. 1a and b). This same technique was also demonstrated using unspun layers of SU-8 approximately 1200 μm thick (Fig. 1c).

Of note, the rough surface of the unspun SU-8 yields smooth and uniform features (Fig. 1d) comparable to traditional photolithography masters. This is made possible by the relatively small effect of film height on resultant channel height especially for very thick SU-8 films (1200 μm) where even substantial (~100 μm) differences in film thickness have negligible effect on resultant channel height. Since UV light exposes the photoresist through the substrate in BDLL, a low amount of UV light is used such that the depth penetration of the UV light is small relative to the film thickness. The roughness of the film surface opposite of the UV light source has no effect on the resultant microchannel. As the UV light is uniformly and carefully controlled with the pGS photomask, uniform channel features can be fabricated from an unspun photoresist layer even with an extremely rough surface. A high-magnification SEM image of the resultant SU-8 molds is included in the electronic supplementary information (ESI† Fig. S1) to demonstrate flatness of resultant channels. At 1200× magnification, it becomes clear that the surface contains dimple-shaped imperfections. The random manner of the imperfections suggests that they arise from UV light diffracted by dust and/or scratches on the UV transilluminator, quartz glass and/or coverglass and not from the repeating binary pattern of opaque and transparent squares.

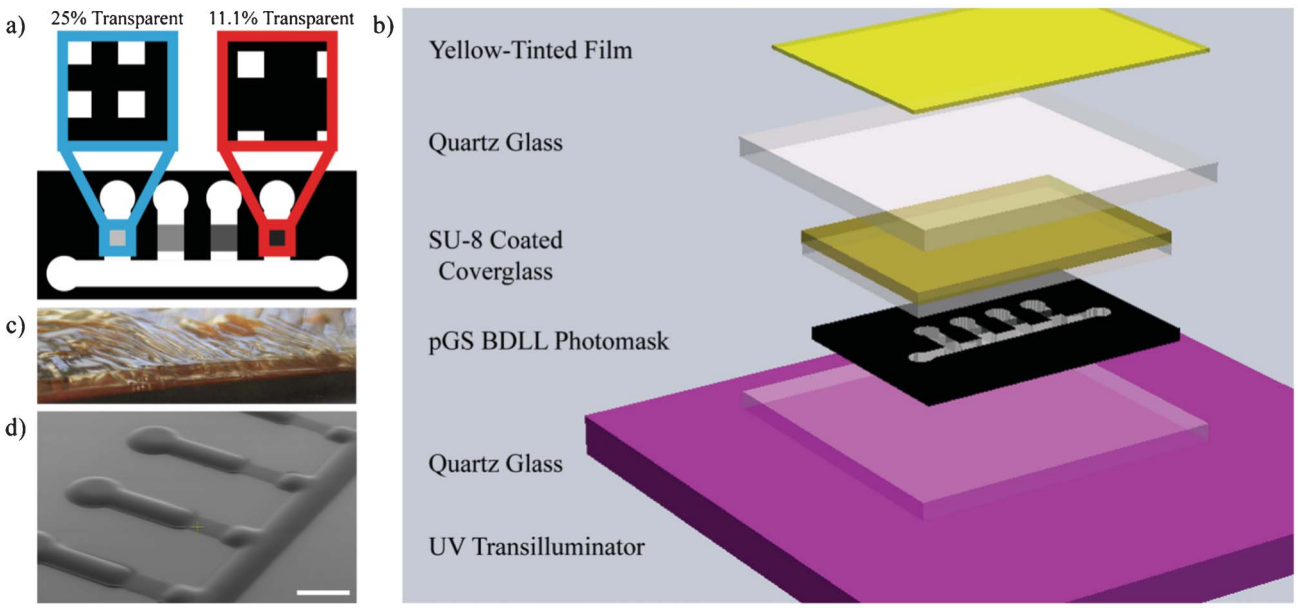

Fig. 1 a) pGS photomask. Binary patterns of transparent/opaque squares produce different levels of ''gray''. Transparent squares are 10 μm by 10 μm. b) Schematic of BDLL. UV light from the UV transilluminator passes through the pGS photomask and glass substrate to expose SU-8 to produce rounded channels of different height depending on how much energy is allowed to pass through the pGS photomask. c) Unspun layer (1200 μm) of SU-8 on glass slide. The surface is crude, normally ineffective for conventional photolithography. d) However, an unspun layer of SU-8 can be used to reliably fabricate multi-layered microfluidic channels using pGS BDLL. SEM image of resultant SU-8 molds. Scale bar: 1 mm.

To demonstrate the utility of pGS BDLL over conventional photolithography, we produced a device to separate red blood cells (RBC) from cancer cells (MDA-MB-231) using nine different levels of per cent transparent to produce an array of weir-type traps of eight different heights (one source channel height and eight weir-trap heights). The equivalent sorter device developed using conventional lithography would require 9 layers of photoresist deposition involving 5 different types of SU-8 photoresist (2075, 2025, 2005, 2002, and 2000.5) and 9 individual spin coating cycles, pre-exposure bakes, UV exposure, and post-exposure bakes.

Fabricated channel height can be finely controlled down to 8 μm by a combination of per cent transparent area of the pGS mask as well as the exposure time of the UV transilluminator. Furthermore, devices designed for cell sorters were fabricated using unspun SU-8 without the use of spin coaters. The effect of exposure time was characterized for each spin height and unspun photoresist thicknesses for 100% transparent photomasks (Fig. 2). Our findings show a relationship between exposure time and channel height and is in agreement with manufacturer specifications for suggested exposure times for conventional photolithography. We discovered that the resultant channel heights are somewhat dependent on film thickness especially at thinner film thicknesses but independent of over-baking during post-exposure bake (data not shown). The effect of pGS BDLL was further characterized by analysing the effect of per cent transparent pGS photomasks for each photoresist thickness and exposure time. Together, these two parameters determine the exposure energy according to eqn (1): $E_{Total} = I_{UV}{}^{*}T^{*}t$, where E_{Total} is the total exposure energy [mJ cm^{-2}], I_{UV} is the intensity of the UV light source [mW cm^{-2}], T is the transparent fraction of the mask [unitless], and t is the exposure time [sec]. For a given film thickness (even unspun layers), exposure energy can be modulated to generate a wide range of feature sizes in a reproducible fashion (Fig. 3).

The usefulness of microfluidics for biological applications is clear, however, the adoption of microfluidic tools by biology labs is stunted by the need for specialized photolithography equipment such as spin coaters and collimated UV light aligners.[27] The characterization of pGS BDLL for the fabrication of microfluidic in this work makes sophisticated multi-level device fabrication accessible to a wide array of biology labs. pGS BDLL only requires hot plates and a UV transilluminator: equipment normally used for DNA and protein analysis and common to most biology labs. The adjustability of pGS BDLL was used to construct weir-type traps for two cell separation applications requiring distinctly different ranges of channel heights.

Cell sorting of MDA-MB-231 cancer cells from red blood cells (RBCs)

Blood analysis of cancer patients for circulating tumour cells (CTCs) is an active area of research with potential for advanced prognosis and identifying individual-specific therapeutic response.[28–30] As such, the effective use of microfluidics for the rapid detection of CTCs within patient blood has high

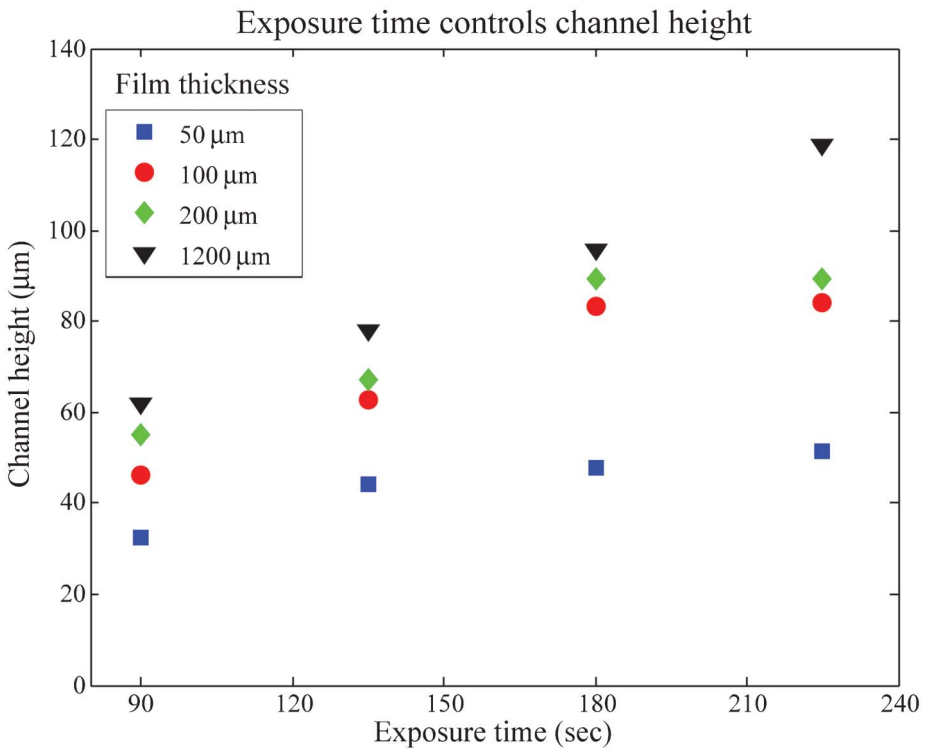

Fig. 2 Using 100% transparent photomasks, different heights can be generated by changing exposure time. The resultant channel height from BDLL is also dependent on SU-8 film thickness.

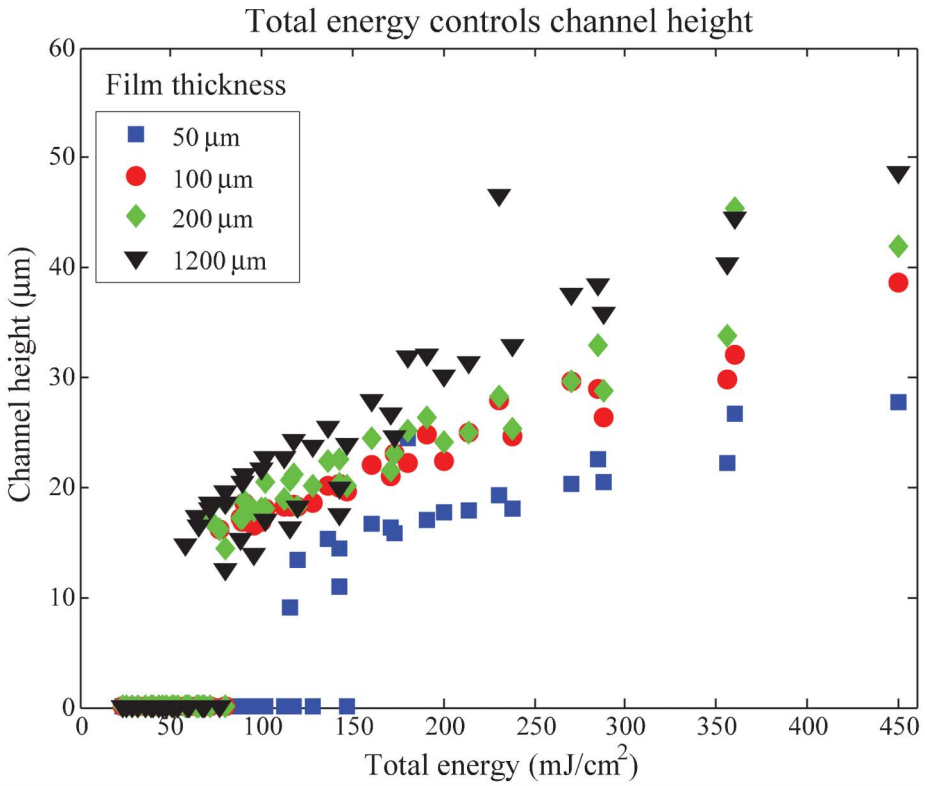

Fig. 3 Using pGS photomasks, the total amount of energy used to expose the photoresist can be controlled using gray scale level and/or exposure time allowing for the fabrication devices with multiple channel heights in a single UV exposure. Total energy is calculated using the percent gray value, exposure time, and the intensity of the UV transilluminator as described by eqn (1).

potential to be a cost-effective method toward fast and individualized patient care.

Motivated by future applications in analyses of blood samples from cancer patients, we used pGS BDLL to generate a mold for soft lithography to produce multiple multi-level PDMS channels simultaneously and inexpensively. A prepared mixture of red blood cells and breast cancer cells were passed through a device with multiple types of weir structures with different sized traps to screen for the optimal structure where cancer cells could be trapped but red blood cells pass through. The effectiveness of the cancer cell trap diminished as the weir-type trap size increased from 8 to 21 μm, where it can no longer trap cells of similar size (Fig. 4).

Cell sorting of murine follicles from stromal cells and MDA-MB-231 cancer cells

Cell-size based separation of different cell types poses a potential application in the field of fertility preservation in cancer survivors. Ovarian tissue can be removed prior to the whole body exposure to toxic chemotherapy, cryopreserved and later transplanted back to the patient to restore fertility. The major drawback of the tissue autotransplantation is the potential risk of reintroduction of cancer cells back to the patient. Ovarian follicles, the functional units of the ovary, can be mechanically or enzymatically isolated from other cell types and transplanted back to the patient as a pure population of the reproductive units using current tissue engineering techniques. With future potential applications of clinical treatment-scale separation of ovarian follicles from cancer cells as a motivation, we used pGS BDLL to create a mold with a wide structure for soft lithography to produce a PDMS device with increased separation capacity to isolate the large ovarian follicles from the smaller cancer cells.

Our design was effective at sorting of follicles from stromal and cancer cells. In these trials, 88% of the cancer cells were removed while 84% of ovarian follicles were recovered, as shown from examination of cell mixture before and after sorting by a microfluidic device (Fig. 5). Our experimental observations suggest a fraction of cancer cells failed to be isolated from follicles due to the cancer cells adhering to the extracellular matrix around the follicles. More experimentation will reveal the collagenase and liberase activity for the optimum cancer cell removal. In a clinically relevant scenario, we anticipate that an 88% contaminant removal may be enough to eliminate all cancer cells.

Disadvantages of pGS BDLL

Despite ease of fabrication of multi-level microchannels using pGS BDLL, it is difficult to stably fabricate microchannel features of width and length <100 μm. Due to the lower adhesion of SU-8 to the glass substrate relative to conventional silicon wafers, features of aspect ratio <1 are easily washed off during development process. Finally, although it is possible to fabricate multi-level microfluidic devices with unspun SU-8

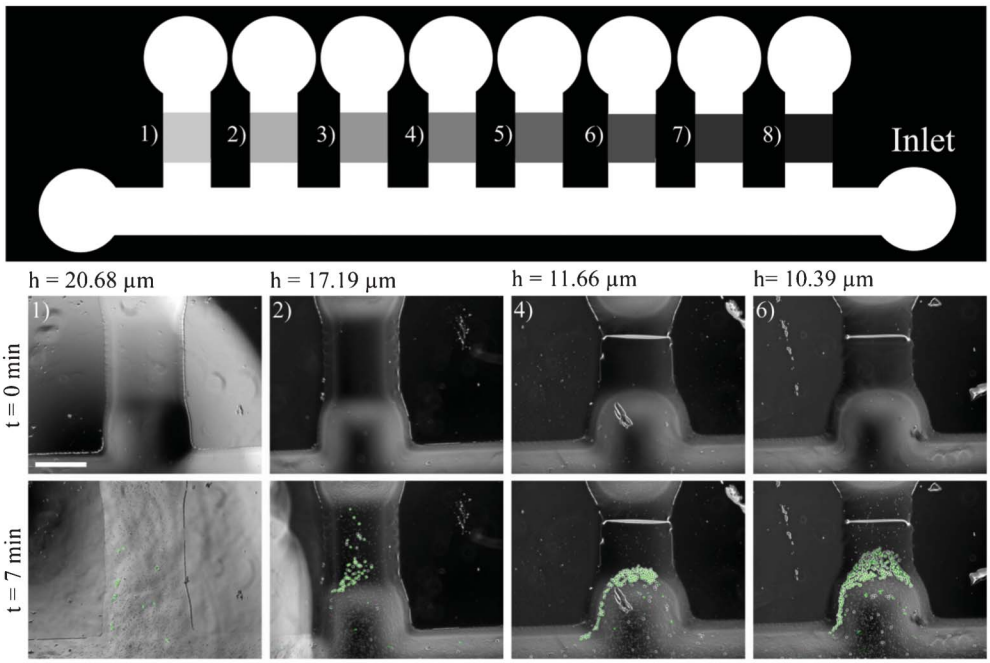

Fig. 4 pGS BDLL was used to produce PDMS microfluidic devices with 8 weir-type traps. PBS containing red blood cells and GFP-MDA-MB-231 cancer cells were passively driven through the weir-type traps by a 3 cm height differential to simulate the trapping and florescence microscopy was used for identification of CTCs trapped within the weir-type traps. The efficiency of weir-type traps depends on the height of the trap produced by pGS BDLL and is evidenced by the slippage and trapping of cancer cells while RBCs are allowed to freely pass through. Each channel is numbered to correspond with its position within the device. Scale bar: 500 μm.

films, the process uses a large amount of negative photoresist. Long and frequent use of pGS BDLL for device fabrication will eventually justify the purchase of a spin coater to decrease SU-8 usage per device fabricated.

Experimental methods

Characterization of pGS BDLL

pGS masks were printed by CAD/Art Services (Bandon, OR) at 20 000 DPI. Individual pseudo-gray areas were created using an isotropic pattern of binary opaque and transparent 10 by 10 μm squares (Fig. 1a). With such patterns, areas of 100%, 25%, 19.8%, 16%, 13.2%, 11.1%, 9.5%, 8.2%, 7.1%, 6.2%, 5.5%, 4.9%, 4.4%, 4%, 3.6% and 3.3% transparent were printed at channel width and length dimensions between 10^2 and 10^4 μm on the photomask for pGS BDLL.

Device fabrication and channel characterization

pGS masks with varying per cent transparent areas were used for BDLL as described previously[22,23] and illustrated in Fig. 1b. Negative photoresist (SU-8 2075 and 2025, MicroChem, Newton, MA) was deposited on coverglass slides at 50 μm, 100 μm, and 200 μm with a spin coater and SU-8 2075 was also deposited onto the same coverglass slides (Fisher Scientific,

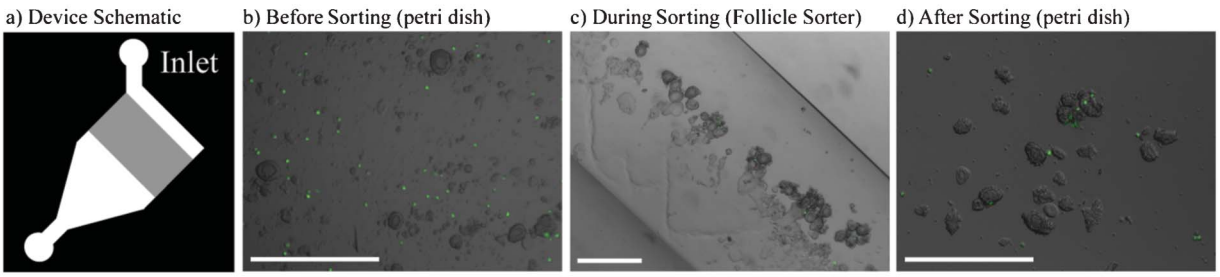

Fig. 5 Follicle sorting from GFP-MDA-MB-231 cancer cells. To further demonstrate the range of possible channel heights and their applications, a separate larger PDMS weir-type trap was produced with unspun SU-8 molds using pGS BDLL. Scale bar: 500 μm. a) Device schematic. b) Cancer cells were added into a solution containing primordial follicles within a petri dish. c) Follicles are trapped by weir-type traps while undigested collagen matrix squeezes through and cancer cells freely pass through. Flow was passive driven by a 7 cm height differential *via* suction of the outlet. d) The trapped follicles can be extracted from the device onto another petri dish by reversing the height differential of the inlet/outlet after a short flushing period with culture medium. The efficiency of cancer cell elimination is 88% and follicle recovery is 84%.

Waltham, MA) without the use of a spin coater to produce a 1200 μm thick layer of photoresist (Fig. 1c).

Each thickness and per cent transparent condition was exposed at four durations: 90 s, 135 s, 180 s, and 225 s on an 8 mW cm^{-2} UV illuminator (816A Ultraviolet Transilluminator, Fisher Scientific, Waltham, MA) to demonstrate the effect of per cent transparent and exposure time and spin/unspun height on resultant channel height on the SU-8 mold. Soft bake, and post exposure bake conditions were controlled according to spin height per manufacturer recommendations. In the unspun condition, since there was no manufacturer recommendation, a soft bake of 15 min at 65 °C and 90 min at 95 °C and a post exposure bake of 10 min at 65 °C and 30 min at 95 °C was used.

Conventional soft lithography was used on these SU-8 molds to produce polydimethylsiloxane (PDMS, Dow Corning, Midland, MI) devices. The resultant PDMS channel heights were determined using light microscopy as well as fluorescence microscopy of channels filled with 0.01% fluorescein as previously described.[23]

MDA-MB-231 cancer cell transfection and cell culture

We previously described MDA-MB-231 human breast cancer cells stably transduced with green fluorescent protein (GFP).[31] Growth media consisted of Dubelco's Modified Eagle Medium supplemented with 10% fetal bovine serum and 1% antibiotic–antimycotic (Life Technologies, Carlsbad, CA). Upon confluence, cells were washed with phosphate buffered saline, trypsinized, resuspended in growth medium, and used in experiments at the concentrations specified.

Enzymatic digestion of ovarian tissue and follicle isolation

For all experiments, we isolated ovaries from 6–8 days old female mice F1 CBA/JxC57BL/6N. Ovaries were extracted and separated from the connective tissues and enzymatically digested in 20 μL (13 Wünsch units per mL) liberase DH (Roche, Indianapolis, IN) in 500 μL L15 (Leibovitz's) media (Sigma-Aldirch, St. Louis, MO). The total digestion time was 1 h at 30 °C and every 15 min, enzyme digested pieces were dispersed by gentle pipetting to isolate follicles.[32] The enzyme digestion was arrested by adding 10% serum and the suspension of the follicles and stromal cells were concentrated to a small volume. Five thousand cancer cells (5 μL of 10^6 mL^{-1} suspension) were added to the follicle-stromal cell suspension to mimic the scenario of cancer cell contaminated tissue. A dramatically higher amount of cancer cells than what is clinically expected was used to facilitate calculation of isolation efficiency.

Red blood cell, cancer cell and follicle sorting

Cells and follicles were sorted using multi-level channels to produce weir-type traps. Devices were fabricated using pGS BDLL with channel heights of 58 μm and weir-type traps of 21 to 8 μm in height for blood sorters and channel heights of 120 μm and 20 μm traps for the follicle sorters. Blood sorting devices were passively driven using a 3 cm positive height differential. The effectiveness of the weir-type trap can be qualitatively observed by MDA-MB-231 cancer cells (at 0.5×10^6 cells mL^{-1}) trapped within the channel while the RBCs (at 2×10^6 cells mL^{-1}, Lampire, Pipersville, PA) are freely allowed to pass through. Follicle sorting devices were driven passively in the form of a suction channel by a 7 cm negative height differential on the opposing end of the weir-type trap to filter 500 μL L15 medium containing ovarian follicles and cancer cells followed by 500 μL L15 media containing no cells to flush most remaining cells and debris through the follicle trap. Ovarian follicles were extracted by reversing the height differential between the inlet and the outlet and collecting ovarian follicles from the inlet in which they were introduced.

Conclusions

Despite the proven usefulness of microfluidics for biological applications, its widespread use is still deterred by the need for specialized equipment needed for photolithography. This work demonstrates a microfluidic device fabrication technique using only equipment commonly found in biology labs. Furthermore, we show the ability of pGS BDLL to fabricate sophisticated multi-level devices that are otherwise highly laborious to create using conventional photolithography. To explore potential cancer research applications as well as to demonstrate the range of structures pGS BDLL is capable of creating, we developed two application specific devices. One is a device with multi-channel, multi-height narrow weir-type traps that can screen designs that are best for trapping metastatic cancer cells in blood while letting red blood cells flow through. Another is a large-width weir-type trap for the isolation of follicle clusters from a mixture that contains unwanted stromal and cancer cells. While our demonstrations focused only on cancer diagnosis and oncofertility preservation, the technique should be broadly useful anywhere rapid prototyping of multi-height microstructures is needed.

Acknowledgements

We thank NIH (CA136829, GM096040) for funding. JML gratefully acknowledges a training grant from the University of Michigan NIH Microfluidics in Biomedical Sciences Training Program (NIH T32 EB005582-05). The authors also thank Jacob Ceccarelli from the Putnam lab at University of Michigan for his assistance with microscopy.

Notes and references

1 A. D. Stroock, *Science*, 2002, **295**, 647–651.
2 P. Wilding, L. J. Kricka, J. Cheng, G. Hvichia, M. A. Shoffner and P. Fortina, *Anal. Biochem.*, 1998, **257**, 95–100.
3 A. M. Skelley, O. Kirak, H. Suh, R. Jaenisch and J. Voldman, *Nat. Methods*, 2009, **6**, 147–152.
4 A. W. Browne, M. J. Rust, W. Jung, S. H. Lee and C. H. Ahn, *Lab Chip*, 2009, **9**, 2941.
5 A. Sayah, P.-A. Thivolle, V. K. Parashar and M. A. M. Gijs, *J. Micromech. Microeng.*, 2009, **19**, 085024.

6 M. L. Kovarik and S. C. Jacobson, *Anal. Chem.*, 2006, **78**, 5214–5217.
7 D. Lim, Y. Kamotani, B. Cho, J. Mazumder and S. Takayama, *Lab Chip*, 2003, **3**, 318.
8 Z. Huang, X. Li, M. Martins-Green and Y. Liu, *Biomed. Microdevices*, 2012, **14**, 873–883.
9 M. E. Wilson, N. Kota, Y. Kim, Y. Wang, D. B. Stolz, P. R. LeDuc and O. B. Ozdoganlar, *Lab Chip*, 2011, **11**, 1550.
10 C. J. Hansen, R. Saksena, D. B. Kolesky, J. J. Vericella, S. J. Kranz, G. P. Muldowney, K. T. Christensen and J. A. Lewis, *Adv. Mater.*, 2013, **25**, 96–102.
11 J. T. Borenstein, M. M. Tupper, P. J. Mack, E. J. Weinberg, A. S. Khalil, J. Hsiao and G. García-Cardeña, *Biomed. Microdevices*, 2009, **12**, 71–79.
12 H. Yu and G. Zhou, *Sensors Actuators B Chem.*, 2013.
13 X. Liu, Q. Wang, J. Qin and B. Lin, *Lab Chip*, 2009, **9**, 1200.
14 V. P. Korolkov, R. Shimansky, A. G. Poleshchuk, V. V. Cherkashin, A. A. Kharissov and D. Denk, ed. E.-B. Kley and H. P. Herzig, 2001, pp. 256–267.
15 B. Wagner, H. J. Quenzer, W. Henke, W. Hoppe and W. Pilz, *Sens. Actuators, A*, 1995, **46**, 89–94.
16 W. Däschner, P. Long, M. Larsson and S. H. Lee, *J. Vac. Sci. Technol., B*, 1995, **13**, 2729.
17 W. Däschner, P. Long, R. Stein, C. Wu and S. H. Lee, *Appl. Opt.*, 1997, **36**, 4675.
18 C. Chen, D. Hirdes and A. Folch, *Proc. Natl. Acad. Sci. U. S. A.*, 2003, **100**, 1499–1504.
19 J. Atencia, S. Barnes, J. Douglas, M. Meacham and L. E. Locascio, *Lab Chip*, 2007, **7**, 1567.
20 J.-H. Lee, W.-S. Choi, K.-H. Lee and J.-B. Yoon, *J. Micromech. Microeng.*, 2008, **18**, 125015.
21 A. Rammohan, P. K. Dwivedi, R. Martinez-Duarte, H. Katepalli, M. J. Madou and A. Sharma, *Sens. Actuators, B*, 2011, **153**, 125–134.
22 N. Futai, W. Gu and S. Takayama, *Adv. Mater.*, 2004, **16**, 1320–1323.
23 D. Lai, J. P. Frampton, H. Sriram and S. Takayama, *Lab Chip*, 2011, **11**, 3551.
24 S. Nagrath, L. V. Sequist, S. Maheswaran, D. W. Bell, D. Irimia, L. Ulkus, M. R. Smith, E. L. Kwak, S. Digumarthy, A. Muzikansky, P. Ryan, U. J. Balis, R. G. Tompkins, D. A. Haber and M. Toner, *Nature*, 2007, **450**, 1235–1239.
25 E. R. West, M. B. Zelinski, L. A. Kondapalli, C. Gracia, J. Chang, C. Coutifaris, J. Critser, R. L. Stouffer, L. D. Shea and T. K. Woodruff, *Pediatr. Blood Cancer*, 2009, **53**, 289–295.
26 J. S. Jeruss and T. K. Woodruff, *N. Engl. J. Med.*, 2009, **360**, 902–911.
27 D. B. Weibel, P. Garstecki and G. M. Whitesides, *Curr. Opin. Neurobiol.*, 2005, **15**, 560–567.
28 J. B. Smerage and D. F. Hayes, *Br. J. Cancer*, 2005, **94**, 8–12.
29 S. Braun and C. Marth, *N. Engl. J. Med.*, 2004, **351**, 824–826.
30 A. Rolle, R. Günzel, U. Pachmann, B. Willen, K. Höffken and K. Pachmann, *World J. Surg. Oncol.*, 2005, **3**, 18.
31 J. W. Song, S. P. Cavnar, A. C. Walker, K. E. Luker, M. Gupta, Y.-C. Tung, G. D. Luker and S. Takayama, *PLoS One*, 2009, **4**, e5756.
32 J. J. Eppig and A. C. Schroeder, *Biol. Reprod.*, 1989, **41**, 268–276.